

# Human Identification Using Multi-region PCA for Iris Recognition

László Lefkovits, Szidónia Lefkovits, Septimiu Crişan, Simina Emerich,

**Abstract**—Biometric identification is a constantly growing field. Many physiological characteristics may be used for reliable identification. The most secure among them uses the iris pattern, because it is unique and stable from eye to eye and from person to person. The approach presented in this article guides through every step of iris-based human identification system from eye localization to iris extraction and identification using PCA features. The novelty of this paper consists of the application of PCA on multi-region iris images. The PCA identification based on multiple regions of interest (ROI) allows higher identification accuracy while extracting much fewer features.

**Keywords**—iris recognition; eigeniris; PCA; performance evaluation; UPOL database

## I. Introduction

Nowadays the increasing security risks and requirements have made human identification essential. Traditional identification and authentication methods can be easily hacked. Token, password or ID-based methods are not sufficiently reliable; tokens, passwords may be intercepted by a man-in-the-middle attack, IDs may be lost and knowledge-based information forgotten. Biometrics is one of the most secure means of personal identification, and methods relying on biometric identification deserve more and more attention. Biometrics makes use of physiological or behavioural characteristics that are difficult to be copied or stolen.

The most important features used in biometric identification are face, fiducial points, fingerprint, vein, palm and dorsal hand vein, finger vein, iris, retina, ear, voice and DNA.

The human iris is one of the most reliable because of its uniqueness and stability; additionally, the non-invasive techniques that prevent falsification ensure accuracy and security.

---

Dr. László Lefkovits

Department of Electrical Engineering  
Sapientia University Țirgu-Mureş, Romania  
Department of Communication  
Technical University Cluj-Napoca, Romania

Dr. Szidónia Lefkovits

Department of Computer Science  
“Petru Maior” University Țirgu-Mureş, Romania

Dr. Simina Emerich and Dr. Septimiu Crişan

Department of Communication,  
Department of Electrical Measurements  
Technical University Cluj-Napoca, Romania

Iris recognition has been and will continue to be widespread in access control, network security, login and authentication, border control and apprehending criminals.

Daugman [1] showed that the iris is the most accurate biometric. The iris is the ringed circular part between the pupil and the sclera. It is made up of connected tissue, is coloured and elastic. Each eye has a unique iris pattern which is different from eye to eye and from person to person. The texture remains the same even if it changes in size. Daugman demonstrated that the probability of finding two people with identical irises is almost zero [2]. Consequently, the iris is the most accurate and reliable biometric feature and is also used in this paper for identification of persons.

This paper is organized as follows: a brief introduction of the field is followed by a short review of the similar biometrics systems based on the iris (section 2). In section 3 the mathematical basis of the PCA method is described, as adapted to iris images. In section 4 the proposed system is presented step by step, followed by results and experiments. Finally, conclusions are drawn and future work is mentioned.

## II. Related Work

The first iris recognition system was proposed by Daugman in [1], and is also known as the conventional system. He uses near-infrared (NIR) iris images. After the preprocessing steps of contrast enhancement and contrast stretching, segmentation is applied. Then the inner and outer boundary of the iris is detected with a circular contour detector. He proposes the “rubber-sheet model” to transform the shrinking or dilating iris ring in a fixed rectangular region. By applying this method, the Cartesian coordinates of the image are converted into polar coordinates, making it rotation-invariant as well. The most important novelty of Daugman’s article was the so-called IrisCode, which is a 256-bit long sequence of 0s or 1s. These represent the signs of the multi-scale 2D Gabor wavelet transform of the normalized image. The matching is based on the Hamming distance of the two-bit sequences obtained after the iris code step.

Aside from the above-mentioned article believed to be the most representative, several other articles were proposed in the literature [3].

In [4], the particle swarm optimization (PSO) method is presented; it localizes the face and inside the face, the iris. This method was compared to the binary edge and intensity-based approach using the SVM classifier. The AdaBoost algorithm, namely the TOBoost (Topology Oriented AdaBoost) was used in [5] to detect the irises inside the face. Eyelid and eyelash-detection improves the reliability of iris detection and its normalization, excluding unwanted, covered regions. In [6] a

parabolic Hough model is combined with Otsu's threshold to detect eyelids and eyelashes on the iris. In [7] the proposed method combines AdaBoost eye detection with iris detection to compensate the error caused by the circular edge detection.

The segmentation step includes the detection of the inner and outer boundaries of the iris, in order to obtain the iris ring. Beside simple circle extraction, regularization (outlier elimination and interpolation of the missing point) may sometimes also be necessary [8].

In the coding step, many features are extracted to create the feature vector of the iris. The 2D Gabor wavelets [2], SIFT [9], DCT (Discrete Cosine Transform) [10], Discrete Fourier Transform [11], Independent Component Analysis [12], Principal Component Analysis [13].

The final step, the recognition or classification step uses several classifiers to identify the persons. In [14] a biorthogonal wavelet network is proposed to classify off-angle irises.

### III. Eigenvalues and Eigenvector for Iris Recognition

The most used global aspect-based method is the Principal Component Analysis. The first application of PCA in visual recognition was implemented by Matthew Turk and Alex Pentland [15] in face classification. From then on, the same idea was used in different domains of object recognition and human identification. The theoretical aspects and the approach were described in detail [16].

The idea of extracting relevant features from a set of training samples can be obtained by the extraction of principal components.

Principal Component Analysis is a statistical technique for reducing dimensionality while minimizing the mean square error between the original and the reconstructed image [17, 18].

The PCA is able to extract the significant information of a given set and transform each of its elements into a lower-dimensional feature-space.

Let us consider  $N$  images, each of them having the width and height  $w \times h$ .

The next step is to compute the covariance matrix of the training set, denoted by  $Tr$ .

$$Tr = \{Img_1, Img_2, \dots, Img_N\} \quad (1)$$

Each image is transformed into the corresponding column vector and we obtain a point set of  $L$ , where  $L = w \times h$ .

The covariance matrix of two random variables e.g. iris images is

$$\Sigma = cov(Img_i, Img_j) = E[(Img_i - \mu_i)(Img_j - \mu_j)] \quad (2)$$

where  $\mu_i = E[X_i]$ ,  $E$  is the expected value of random variable  $Img_j$ .

The eigenvalues and eigenvectors of the covariance matrix  $\Sigma$  are obtained, these will be called eigenirises.

The problem is the dimension of the covariance matrix  $\Sigma$ , which becomes  $L^2 \times L^2$ .  $L$  is the number of unknowns in the characteristic equation denoted by equation (3), used to find the eigenvalues  $c$  of matrix  $M$ .

$$\det(M - cI_n) = 0 \quad (3)$$

where  $M$  is an  $L^2 \times N$  matrix having  $N$  columns, that are formed of the differences of each image and the mean image, the  $i$ th column is the  $i$ th difference.

$$M = [I_1 - \mu \ I_2 - \mu \ \dots \ I_L - \mu] \quad (4)$$

Luckily, the same eigenvalues are obtained by computing them for another covariance matrix. This covariance matrix is

$$\Sigma' = M^T M, \quad (5)$$

The dimension of this  $\Sigma'$  matrix is  $N \times N$ , where  $N$  is the total number of iris images. The order of magnitude of  $L^2$  is million, but the order of  $N$  is 256 in the case of the UPOL database ( $N \ll L^2$ ).

We obtain the eigenvalues  $c_i$  and eigenvectors  $u_i$  of the  $\Sigma$  covariance matrix or the same eigenvalues and eigenvectors are obtained if we compute them for  $\Sigma'$ .

After computing all the  $N$  eigenvalues, we have to select the first  $n$  eigenvalues. This value of  $n$  is less than hundred.

From the total number of  $N$  eigenvalues, the largest  $n$  eigenvalues are considered and the corresponding eigenvectors are computed using this formula

$$Mv_i = c_i v_i \quad (6)$$

The training step is the computation of the new feature-space based on the most representative  $n$  eigenvectors.

In the testing phase, the new image must be projected onto the new feature space.

Each of the first  $n$  eigenvectors will have a corresponding weight. These weights are the coefficients of the eigenvectors  $v_i$ . The linear combination of these vectors forms the reconstructed image in the new space. Every weight is obtained by the formula,

$$w_n = v_n^T (Img_{input} - \mu) \quad (7)$$

The weights are put together column-wise to form the final weight-matrix.

$$W = [w_1, w_2, \dots, w_n]. \quad (8)$$

In order to determine which iris resembles the test image best, an error must be computed. This error is the mean square error of two  $W$  matrixes [17].  $W_{test}$  is the weight matrix of the test iris image and  $W_{ID}$  is the average weight matrix of more images for a given person having the same ID.

$$RMSE = \|W_{test} - W_{ID}\| \quad (9)$$

The minimum of this mean square error will determine the most similar iris pair.

If the error is greater than a threshold ( $T$ ), we can say that the input iris image belongs to an unknown person.

### IV. Results and Experiments

The main phases of the most common iris recognition systems are the following: (1) iris image acquisition, (2)

detection and localization, (3) iris segmentation, (4) image enhancement, (5) preprocessing, (6) normalization, (7) feature extraction, (8) matching, (9) recognition and identification [3].

The detection and localization of the face and the eye is indispensable in an iris-based human identification system. In our case the face detection and eye localization parts were presented in our previously published articles. The face detector was an enhanced Haar-like feature-based object detector with the GentleBoost algorithm.

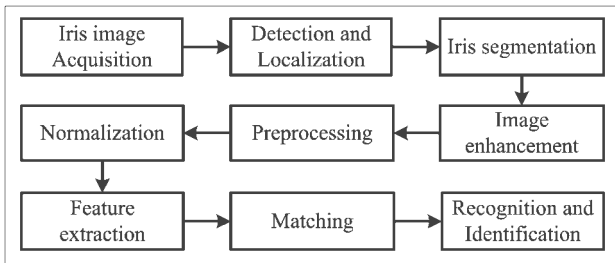


Fig. 1. Block diagram of the proposed approach

It has a detection rate comparable to the well-known Viola Jones system [18], but it manages to eliminate more false detections. For more details see [19].

The eye detection step was presented in [20, 21]. The approach is based on the computation of multi-scale Gabor wavelets. These filter responses were classified by different types of boosting algorithms. Unfortunately, in the case of face and eye localization the eyes were of only 16×16 size. These small eye regions are not adequate for iris recognition. Hence, we have decided to use our proposed method on different eye images. But if there were a publicly available face database that was also suitable for iris recognition, the entire approach could be applied to the same images from face and eye detection to iris localization and biometric identification.

In the following we present our approach, going through steps (1) to (9) from Fig. 1.

Thus, the iris images are considered to be ready for use in identification. In our experiments, we have used the UPOL database. The images in this database were acquired by the University of Palackeho and Olomouc [22]. It contains 384 colour images of both eyes (3 images for the left eye and 3 images for the right eye) from 64 subjects. The resolution of every image is 768×576 pixels. The images, acquired by an optometric device connected to a Sony DXC-950P, are noiseless (Fig. 2).

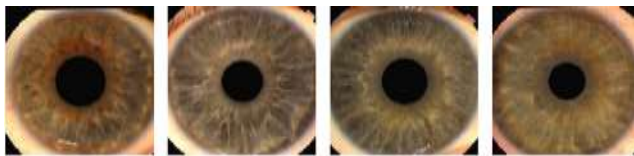


Fig. 2. Sample from the UPOL database

The second step was iris segmentation. After converting the

24-bit .png image (Fig. 3a) into greyscale, the pupil (interior boundary of the iris) and the exterior boundary of the iris were detected in multiple consecutive preprocessing steps. The contrast of the original image was enhanced by histogram equalization. The Canny edge detector was applied in the image obtained to detect contours (Fig. 3b). We also computed the optimal threshold to detect the mask which was being considered. The mask was obtained by computing Ostu's threshold twice; first for delimiting the background from the eye, and second for delimiting the pupil from the iris (Fig. 4a). Based on the contours obtained, the Hough transform [7] (Fig. 4b) was applied for circles in order to detect the inner and outer border of the iris. Applying the gradient filter or the edge detector on the image before the Hough transform computation shortens computation time significantly, because only the edge points are being taken into consideration and accumulated in the accumulator table of a given pair of  $(\rho, \theta)$  parameters.

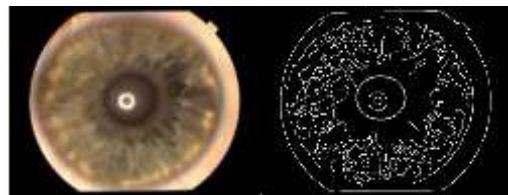


Fig. 3. a) Original image b) Canny edges



Fig. 4. a) Otsu mask b) Hough transform

The normalization process converts the ring-like iris region into a rectangular region with the same dimension. This procedure ensures that the same iris taken in different lighting conditions will have the same features at the same spatial locations. The most well-known method of normalization is Daugman's rubber sheet model [1]. It maps every pair of points in the Cartesian coordinates to the corresponding polar coordinates.

The advantage of this model is that it compensates for pupil dilation and non-concentric pupil displacement.

Applying the method presented above, we obtained rectangular iris images of 1600×180 pixels. Fig. 5 shows the ring-like iris image and the normalized image of 2×800×180 obtained. The feature extraction, image matching and identifications steps are done via the previously described PCA method (Section 3). The grayscale image of the rectangular normalized images was used for all subsequent steps. The PCA begins with the computation of the mean image (fig. 6a) of the entire training dataset.

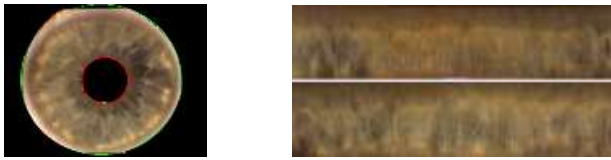


Fig. 5. a) Iris ring b) Rubber sheet of the same iris

According to the covariance and similarity between the images, this mean image represents the common part of the training set, which is why it must be subtracted from every image in the training set (fig. 6b). In addition, the difference images are enhanced using histogram equalization (see fig. 6c).

After computing the difference images, the computation of the covariance matrix is performed used to obtain the eigenvalues and eigenvectors.



Fig. 6. a). Mean image denoted by  $\mu$  b). Difference image c) Histogram-equalized difference image



Fig. 7. First three eigenirises



Fig. 8. 48th, 49th, 50th

In our experiments, we studied the influence of the number of eigenvectors used on iris decomposition. We have created the orthogonal basis of eigenvectors using 25, 50, 75, 100, 125 and 256 eigenvectors corresponding to the most representative eigenvalues. Fig. 7 shows the eigenvectors corresponding to the most representative (first three) eigenvalues. These images are the coarse representation of the iris patterns. Compared to these, the last three eigenvectors (48<sup>th</sup>, 49<sup>th</sup>, 50<sup>th</sup> - fig. 8) are the fine details extracted from the training dataset. In order to

obtain a proper reconstruction, several coarse eigenvectors are necessary, but the eigenvectors corresponding to the fine contours are also indispensable.

In Table 1 we measured the recognition rate using 25, 50, 75,100, 125, 256 eigenvectors.

The best detection rate is achieved between 75-100 eigenvectors, yielding a detection rate of 99%. Table 1 shows that after 100 eigenvectors, considering more eigenvectors is useless. In the testing phase, each evaluated image is compared to the existing classes in the training set (64 subjects  $\times$  2 images  $\times$  2 eyes). Each class corresponds to a certain person. For each image in the training set, we compute its weight. This weight is the dot product of the difference image  $\text{Img}_{input} - \mu$  and the eigenvectors  $u_p$  (equation (7)). After computing the weights for the training images, the weights are averaged over each individual.

TABLE I. RECOGNITION ACCURACY VS. NO. OF EIGENVECTORS

No. of eigenirises	Recognition accuracy One eye	Recognition accuracy Both eyes
25	78%	87%
50	92%	98%
75	97%	99%
100	99%	100%
125	99%	100%
256	100%	100%

The root-mean-square error (RMSE) of the reconstruction is computed between the average weight vector of the training images and the test image (equation (9)). The more eigenvectors are included, the better the accuracy, but the dimensionality of the obtained weight-vectors also becomes higher. The RMSE can also be expressed visually; it is the difference between the original image and the reconstructed image, with  $n=25$ ,  $n=50$ ,  $n=75$ ,  $n=100$  eigenvectors (Fig. 9).



Fig. 9. Reconstructed irises with 25 and 50 eigenvectors

In order to reduce the number of eigenvectors used, we created a two-step recognition system: different training for the left eye and different training for the right eye. In the test phase, we compared both eyes to both eyes of the individuals in the training set. By double-checking the correct identification, we obtained a 97% detection rate at only 50 eigenvectors, and a 99% accuracy at 75 eigenvectors (Table I column 3.)

Our third experiment was related to the size of the rectangular ROI of the iris. We were able to reduce the analysed zone, split the rectangle into 2 pieces of 700 $\times$ 150 ROI, and subsequently, 4 pieces of 350 $\times$ 150 ROI.

TABLE II. RECOGNITION ACCURACY VS. NO. OF EIGENVECTORS

No. of eigenirises	Resolution	Recognition accuracy One eye	Recognition accuracy Both eyes
25	1400×150	78%	84%
25	2×700×150	96%	100%
25	4×350×150	100%	100%
50	1400×150	92%	97%
50	2×700×150	99%	100%
50	4×350×150	100%	100%
75	1400×150	97%	99%
75	2×700×150	100%	100%
75	4×350×150	100%	100%

This way, the size of the training set became half or one quarter the size of the original training set, but the PCA extraction procedure has to be applied twice or four times. Recognition and identification results demonstrate that the system proposed does not have to analyse the entire iris; it is sufficient to extract merely a given part of it. Furthermore, it is recommended to analyse different parts of the iris independently. Thus, the final identification step can be done by a weighted voting procedure, taking the RMSE of different iris parts into consideration.

The recognition and identification accuracy of the combined iris parts are given in Table II. If the iris is split into more pieces and the recognition takes into consideration all 4 regions separately, the number of necessary eigenvectors can be significantly reduced, and the recognition rate is 100% in the case of the database studied.

## v. Conclusion

In this paper, we propose a human identification system based on iris biometrics. The approach created uses preprocessing steps to extract the iris. The ring region is normalized to obtain a fixed rectangular image. This way the images are aligned and the PCA features can be extracted accurately. The novelty of this work consists of the multi-scale PCA extraction that ensures multiple identifications based on different iris parts considering both eyes. Multi-resolution identification allows us to extract fewer features and to maintain the same identification accuracy.

Overall, these observations can be helpful in designing future biometric identification systems based on the data fusion of several biometric markers such as face, iris, palm or dorsal vein.

## Acknowledgment

This work was supported by a grant of the Romanian National Authority for Scientific Research and Innovation, CNCS – UEFISCDI, project number PN-II-RU-TE-2014-4-2080.

## References

- [1] J. G. Daugman, "High confidence visual recognition of persons by a test of statistical independence," IEEE transactions on pattern analysis and machine intelligence, vol. 15, pp. 1148-1161, 1993.
- [2] J. Daugman, "How iris recognition works," IEEE Transactions on circuits and systems for video technology, vol. 14, pp. 21-30, 2004.
- [3] K. Nguyen, C. Fookes, R. Jillela et al., "Long range iris recognition: A survey," Pattern Recognition, vol. 72, pp. 123-143, 2017.
- [4] C. A. Perez, C. M. Aravena, J. I. Vallejos, P. A. Estevez and C. M. Held, "Face and iris localization using templates designed by particle swarm optimization," Pattern Recognition Letters, vol. 31, pp. 857-868, 2010.
- [5] Z. He, T. Tan and Z. Sun, "Topology modeling for Adaboost-cascade based object detection," Pattern Rec. Letters, vol. 31, pp. 912-919, 2010.
- [6] T.-H. Min and R.-H. Park, "Eyelid and eyelash detection method in the normalized iris image using the parabolic Hough model and Otsu's thresholding method," Pattern Rec Letters, vol. 30, pp. 1138-1143, 2009.
- [7] D. S. Jeong, J. W. Hwang, B. J. Kang, K. R. Park, C. S. Won, D.-K. Park and J. Kim, "A new iris segmentation method for non-ideal iris images," Image and Vision Computing, vol. 28, pp. 254-260, 2010.
- [8] R. D. Labati and F. Scotti, "Noisy iris segmentation with boundary regularization and reflections removal," Image and Vision Computing, vol. 28, pp. 270-277, 2010.
- [9] G. Yang, S. Pang, Y. Yin, Y. Li and X. Li, "SIFT based iris recognition with normalization and enhancement," Int. Journal of Machine Learning & Cybernetics, vol. 4, pp. 401-407, 2013.
- [10] D. M. Monro, S. Rakshit and D. Zhang, "DCT-Based Iris Recognition," Pattern Analysis and Machine Intelligence, vol. 29, pp. 586-595, 2007
- [11] K. Miyazawa, K. Ito, T. Aoki, et al., "An Effective Approach for Iris Recognition Using Phase-Based Image Matching," IEEE Tr. on Pattern Analysis and Machine Intelligence, vol. 30, pp. 1741-1756, 2008
- [12] Y.-P. Huang, S.-W. Luo and E.-Y. Chen, "An efficient iris recognition system," Int. Conf. on in Machine Learning and Cybernetics, 2002.
- [13] J.-X. Shi and X.-F. Gu, "The comparison of iris recognition using principal component analysis, independent component analysis and Gabor wavelets," in Int. Conf. on Computer Science and Information Technology, 2010.
- [14] A. Abhyankar and S. Schuckers, "A novel biorthogonal wavelet network system for off-angle iris recognition," Pattern Recognition, vol. 43, pp. 987-1007, 2010.
- [15] M. Turk and A. Pentland, "Eigenfaces for recognition," Journal of cognitive neuroscience, vol. 3, pp. 71-86, 1991.
- [16] S. Lefkovits and L. Lefkovits, "Performance Analysis of Eigenface Recognition Under Varying External Conditions," Scientific Bulletin of the "Petru Maior" University, vol. 11, pp. 44-49, 2014.
- [17] B. Poon, M. Ashraf Amin and H. Yan, "Performance evaluation and comparison of PCA Based human face recognition methods for distorted images," Int. Journal of Machine Learning and Cybernetics, vol. 2, pp. 245-259, 2011.
- [18] V. Hiremath and A. Mayakar, "Face Recognition Using Eigenface Approach," in IDT workshop on interesting results in computer science and engineering Sweden, 2009.
- [19] P. Viola, M. and J. Jones, "Rapid object detection using a boosted cascade of simple features," in Computer Vision and Pattern Recognition (CVPR), 2001.
- [20] S. Lefkovits, "Novel Gabor filter-based patch descriptor," in IEEE 10th International Symposium Intelligent Systems and Informatics, 2012.
- [21] S. Lefkovits, L. Lefkovits and S. Emerich, "Detecting the eye and its openness with Gabor filters," in 2017 5th International Symposium on Digital Forensic and Security (ISDFS), 2017
- [22] M. Dobs and L. Machala, UPOL Iris Database. <http://phoenix.inf.upol.cz/iris/>